ORGANOMETALLICS

pubs.acs.org/Organometallics

Communication

Methyl-Branched Polyethylene Produced by Hafnocene Complexes Exhibiting Unconventional Dialkoxy Bridges

Tim M. Lenz,[†] Juliana Steck,[†] Jin Y. Liu, and Bernhard Rieger*

Cite This: *Organometallics* 2025, 44, 8–13

Read Online

ABSTRACT: Research on the homogeneous polymerization of propylene employing group IV metallocene complexes primarily focuses on structures like *rac*-dimethylsilanediylbis(4-phenyl-7-methoxy-2-methylindenyl)hafnium dichloride (*rac*-**I**), featuring the long-established *Spaleck*-type $-SiMe_2-$ bridge between two indenyl fragments, while such complexes are rarely used in ethylene polymerization. This work describes the syntheses and polymerization performances of two hafnocene complexes, *rac*-ethane-1,2-diyl((2-methyl-7-phenyl-1*H*-inden-4-yl)oxy)hafnium dichloride (*rac*-**II**) and *rac*-propane-1,3-diyl((2-methyl-7-phenyl-1*H*-inden-4-yl)oxy)hafnium dichloride (*rac*-**III**), bearing unconventional dialkoxy bridges of varying lengths. Single-crystal X-ray diffraction experiments enabled the comparison of characteristic geometric parameters between the two synthesized hafnocenes and *Spaleck*-type complex *rac*-**I**. Upon activation with different cocatalysts, *rac*-**II** and *rac*-**III** yielded polyethylene with exclusively methyl branches, contrary to long-chain branches, which are usually formed when group IV metallocene complexes are applied for ethylene polymerization. Thus, a branching mechanism related to the prominent chain-walking mechanism, which is frequently observed for late transition-metal complexes, is proposed. Furthermore, the degree of branching could be regulated by adjusting the employed cocatalysts, polymerization temperatures, and bridge lengths, allowing the control of the polymers' melting transition temperatures.

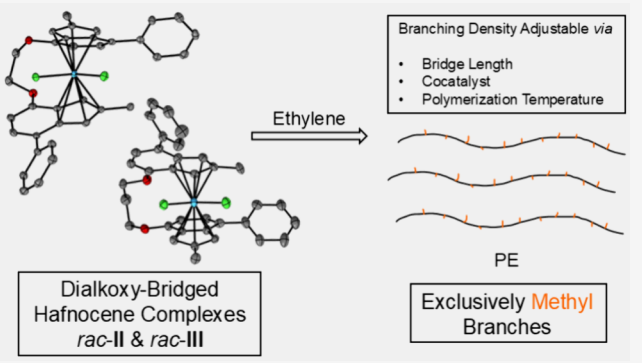

Ever since the discoveries of *Brintzinger* and *Kaminsky*, who showed that *racemic* (*rac*) *ansa*-metallocene complexes yielded isotactic polypropylene (iPP) when activated with methylaluminoxane (MAO),[1−3] a plethora of different precatalysts were synthesized and reported, allowing precise tailoring of the macromolecular characteristics of polyolefins.[4] Most of these complexes, particularly those reported in the last two decades, share the common motif of a $-SiMe_2-$ group bridging two indenyl ligands,[5−10] tremendously increasing the catalysts' activities compared to the original ethylene-bridged systems.[11] In 2012, our group designed an ultrarigid hafnocene complex, which yielded perfectly isotactic PP with a melting transition (*ex reactor*) of 171 °C—the highest reported one to this date.[8] The synthesis of its structural relative **I** (Scheme 1) was carried out in 2017.[7] Recently, we discovered that the methoxy groups of these complexes enabled an unprecedented *in situ* isomerization of their *meso* isomers to their *rac* analogues, which drastically improved the overall yield of iPP per mole of metallocene.[12,13] Curious about the catalytic properties of analogue complexes where these methoxy groups are repurposed as *ansa*-bridges linking both indenyl fragments, we set out to synthesize the hafnocenes **II** and **III** (Scheme 1). Since we found that the methoxy groups of **I** rendered its *rac* isomer thermodynamically far more stable than the *meso* one,[12] we initially expected such a bridge to suppress the formation of the latter, making a tedious isomer separation obsolete.

Starting from indanone **1**,[8] the syntheses of **II** and **III** were achieved in four steps, each. In the first step, the alkyl bridge, connecting both ligand fragments and consisting of two or three methylene units, respectively, was introduced via a *Mitsunobu* reaction, yielding the indanones **2**. Attempts to bridge both indanones using dihalo-alkanes, such as 1,2-dibromoethane, only led to monosubstituted alkyl halides, which were presumably too bulky to undergo the necessary substitution of a second halide with **1**. Reduction of **2** to the corresponding bridged bis(indanols) and subsequent elimination of water yielded the indenes **3** which were converted to the ligands **4** via a *Negishi* cross-coupling reaction. Deprotonation followed by salt metathesis with $HfCl_4$ resulted in the formation of targeted hafnocene complexes **II** and **III** (Scheme 1).

Received: October 29, 2024
Revised: December 18, 2024
Accepted: December 27, 2024
Published: December 31, 2024

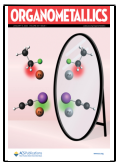

Scheme 1. Synthetic Routes toward the Hafnocene Complexes *rac*-II and *rac*-III[a]

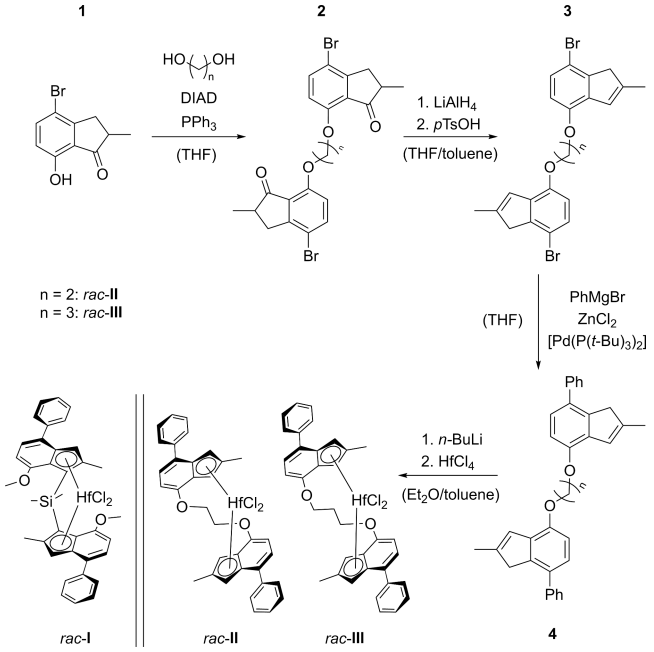

[a]For *rac*-I see ref 7.

^{1}H nuclear magnetic resonance (NMR) analysis of the crude reaction products revealed the presence of both *rac* and *meso* isomers of **II** (ratio 1:1) and **III** (ratio 3:2), although dialkoxy bridges were initially introduced to prevent the formation of the latter. Therefore, we assume that *meso*-**II** and *meso*-**III** are the kinetically favored products of the salt metathesis step, possibly being formed due to some kind of oxygen−lithium coordination in the deprotonated bis(indenyl) precursors. Fractional crystallization of the isomeric mixtures from toluene yielded pure *rac*-**II** and *rac*-**III**, respectively. Single-crystal X-ray diffraction (SC-XRD) confirmed that both species were obtained as *rac* isomers (Figure 1). Characteristic angles and distances in the solid-state structures of *rac*-**I**, *rac*-**II**, and *rac*-**III** are summarized in Table 1.

Table 1. Selected Bond Distances and Characteristic Angles in the Solid Structures (*rac*-I, *rac*-II, *rac*-III) according to *Rath* and *Coville*[7,14,15]

complex	bite angle (deg)	dihedral angle (deg)	Hf-$Cp_{centroid}$ (Å)	*D* (Å)
rac-**I**	58.9	41.1/45.2	2.224 ± 2	0.949 ± 4
rac-**II**	48.2	39.3/43.5	2.222 ± 2	0.882 ± 4
rac-**III**	48.0	38.2/45.3	2.225 ± 1	0.904 ± 3

Both *rac*-**II** and *rac*-**III** exhibit a bite angle between both cyclopentadienyl (Cp) units that is almost 11° lower than the one of *rac*-**I**, while other characteristic values, such as Hf-Cp distances, dihedral angles, and *D* values, do not significantly differ between the three structures.[7,14,15] This divergence evidently originates from the former complexes lacking a −$SiMe_2$− bridge. In general, −$SiMe_2$− bridges are specifically introduced into the frameworks of metallocenes to increase their bite angles and, thus, deshield their central metal atoms.[16] This facilitates the coordination of sterically more demanding olefins, and typically higher chain propagation rates during polymerization are accomplished.[11]

In line with the previous findings, activation of *rac*-**II**/*rac*-**III** with triisobutylaluminum (TIBA) and $[Ph_3C][B(C_6F_5)_4]$ (TrBCF), followed by the exchange of the argon atmosphere with propylene (1 bar) in a *J. Young* NMR tube, led to rather slow consumption of the monomer—90 min for *rac*-**III** and 180 min for *rac*-**II** at 100 °C (Figures S1 and S2). Analogous experiments using *Spaleck*-type catalysts, instead, caused propylene to be consumed within a few seconds, already at room temperature.[17,18] Even autoclave polymerizations at a pressure of 4 bar did not yield polypropylene in quantities suitable for molecular weight, tacticity, and melting transition temperature analysis. Higher pressures might resolve this issue, but unfortunately, the pressures were limited by our experimental setup. However, *rac*-**II** and *rac*-**III** proved to be highly efficient ethylene polymerization catalysts—entries 1−5

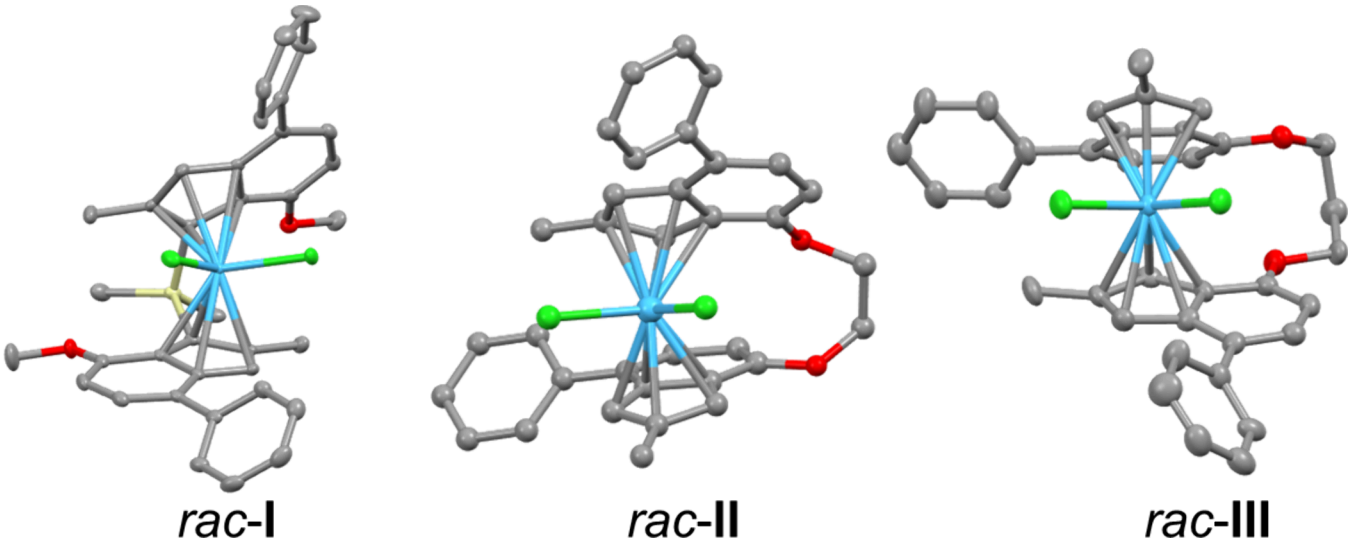

Figure 1. ORTEP style representation of *rac*-**I**, *rac*-**II**, and *rac*-**III** with ellipsoids drawn at the 50% probability level. Hydrogen atoms are omitted for clarity.[7]

https://doi.org/10.1021/acs.organomet.4c00459
Organometallics 2025, 44, 8−13

Table 2. Conditions and Results[a] for the Polymerization of Ethylene with Complexes *rac*-II and *rac*-III, as well as the "Standard" Zirconocene Complex Et[H_4Ind]$_2$ZrCl_2 for Comparison[20]

entry	complex	n^b	cocatalyst[c]	T_{Polym}[d]	M_W[e]	$Đ$[f]	T_m[d]	P[g]	branch density[h]
1	*rac*-**II**	4.18	TIBA/TrBCF	30	290 000	10.0	128	17	16
2	*rac*-**II**	4.18	TIBA/TrBCF	90	57000	3.0	127	1400	9
3	*rac*-**III**	4.10	TIBA/TrBCF	30	16000	2.7	118	160	66
4	*rac*-**III**	4.10	TIBA/TrBCF	90	17000	3.8	114	1200	104
5	*rac*-**III**	4.10	Al−H−Al	30	3500	3.4	123	400	43
6[20]	Et[H_4Ind]$_2$ZrCl_2	2.00	MAO	80	114 000	2.1	n.d.	2900	25

[a]Entries 1−5: $V_{toluene}$ = 120 mL; $p = p_{Ar} + p_{ethylene}$ = 4.0 bar; t_{Polym} = 30 min. [b]In μmol. [c]TIBA/TrBCF: initiator [Ph_3C][B(C_6F_5)$_4$] = 5 equiv, activator (TIBA) = 60 equiv, scavenger (TIBA) = 0.25 mmol; Al−H−Al: scavenger = activator [(*i*-Bu_2(DMA)Al)$_2$(μ-H)][B(C_6F_5)$_4$] = 30 equiv.[25] [d]In °C. [e]In g mol^{-1} determined via SEC-GPC in 1,2,4-trichlorobenzene at 160 °C against a narrow PS standard. [f]$Đ = M_W/M_n$. [g]In kg_{PE} [mol_{cat} h]$^{-1}$. [h]In ‰ determined through integration of the CH_2 versus CH_3 signals in the ^{1}H NMR spectra according to ref 19.

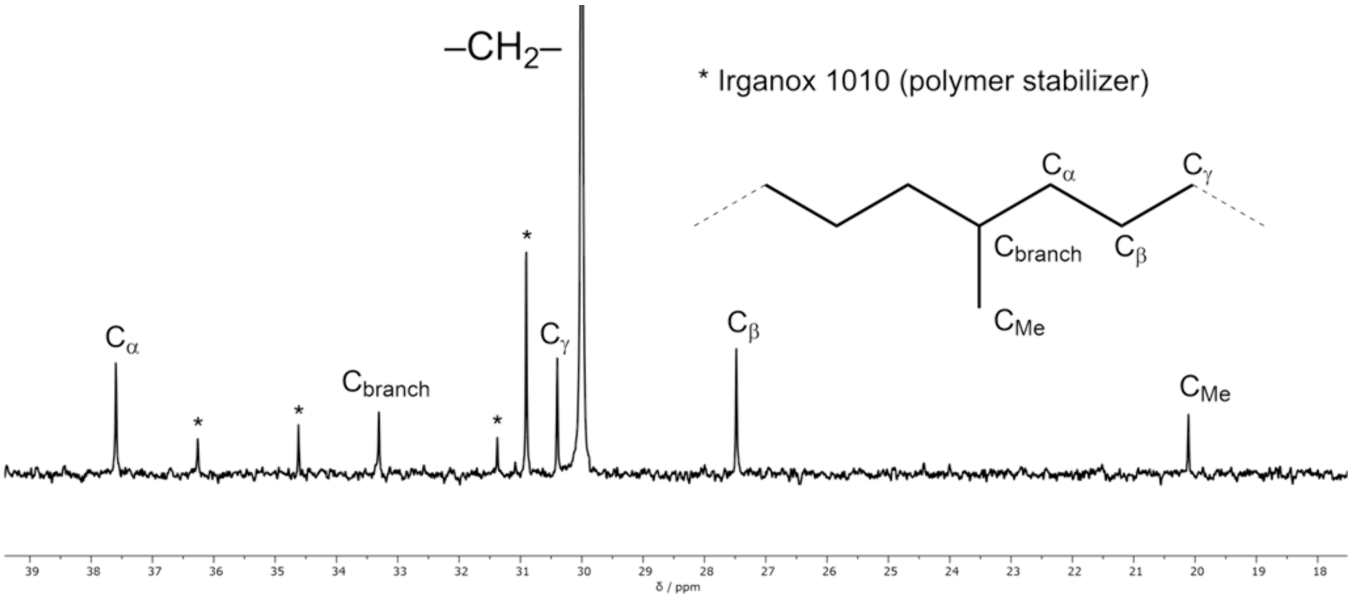

Figure 2. Excerpt of the ^{13}C NMR spectrum of entry 4 (Table 2) with carbon atoms assigned according to their chemical shifts.[20,21] Signals marked with an asterisk correspond to residual Irganox 1010 (polymer stabilizer).[13]

of Table 2 summarize the macromolecular characteristics of polyethylene (PE) produced with both hafnocene complexes. For comparison, entry 6 lists the analogous properties of PE obtained with the "standard" zirconocene complex Et-[H_4Ind]$_2$ZrCl_2, which has previously been observed to cause high degrees of methyl-branching.

The data summarized in Table 2 indicate two trends: Both hafnocenes, *rac*-**II** and *rac*-**III**, became significantly more productive at higher polymerization temperatures, and PE produced by *rac*-**III** exhibited higher degrees of branching.[19] Taking the poor propylene polymerization activity and the low bite angle of both complexes into account, we anticipate the first trend is quite anticipated. At low polymerization temperatures, coordination of ethylene to the rather shielded central metal atom simply appeared to occur at a very slow rate. The discrepancies in PE branching, induced by the different hafnocenes, however, require a more in-depth examination. ^{13}C NMR analysis of the polymers revealed that all branches consist solely of methyl groups (Figure 2).[20] We hypothesize that these branches are formed via β-H elimination of growing polymeryl chains, resulting in vinyl-terminated PEs and the respective metal-hydride complexes. Subsequent 2,1-reinsertion and further chain propagation exclusively yields methyl branches.[21,22]

The branching mechanism, which is usually observed for group IV metallocene complexes, consists of the insertion of vinyl-terminated PEs into other growing polymeryl chains, leading to long-chain branched PE.[23,24] As shown by the propylene polymerization experiments mentioned above, *rac*-**II** and *rac*-**III** were quite inefficient at inserting α-olefins. It seems that both complexes were unable to incorporate vinyl-terminated PEs into growing polymeryl chains and, thereby, did not produce long-chain branched PE. The mechanism observed for *rac*-**II** and *rac*-**III** rather reminds of a chain-walking mechanism, which is frequently observed for late transition-metal catalysts, such as α-diimine Ni or Pd complexes reported by the groups of *Brookhart* and *Guan*.[26−28] Herein, β-H elimination and subsequent reinsertion with opposite regiochemistry compete with chain propagation at any time of the reaction, thus yielding PE with higher or lower branching densities, dependent on ligand structures, as well as polymerization conditions.[29,30] Evidently, *rac*-**II** and *rac*-**III** did not facilitate a second β-H elimination subsequent to a 2,1-insertion, which is why they exclusively yielded PE with methyl branches—therefore the observed mechanism is better described as a type of *restrained* chain-walking (Scheme 2). Parallels to α-diimine Ni complexes become even more evident when considering that suitable

https://doi.org/10.1021/acs.organomet.4c00459
Organometallics 2025, 44, 8−13

Scheme 2. Proposed β-H Elimination/2,1-Reinsertion Mechanism Yielding Methyl Branches[a] upon Ethylene Polymerization Employing *rac*-II and *rac*-III[21,29]

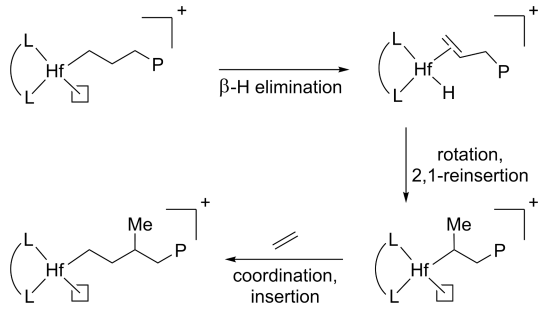

[a]L: ligand; P: polymeryl.

ligand substitution in such complexes can similarly promote the formation of methyl branches.[31,32]

Taking into account the proposed branching mechanism exhibited by *rac*-**II** and *rac*-**III**, the aforementioned differences in the branching densities of PE generated by either can be explained. According to the data presented in Table 2, *rac*-**III** produced PE with significantly more branches than *rac*-**II** under equal polymerization conditions, i.e., polymerization temperature, employed cocatalyst, and monomer pressure (entries 1/3 and 2/4, Table 2). Simultaneously, the polymers produced by *rac*-**II** exhibited higher average molecular weights. Thus, it seems that β-H elimination—and consecutive 2,1-reinsertion—is promoted by *rac*-**III**, whereas it is suppressed by *rac*-**II**. This observation is further evidenced by the varying molecular weights of PE produced at different polymerization temperatures: While a temperature increase barely influences the molecular weight of PE produced by *rac*-**III** (entries 3/4, Table 2), the molecular weight of PE produced by *rac*-**II** at higher temperatures is significantly lower (entries 1/2, Table 2). These data highlight that β-H elimination with *rac*-**II** leads to chain termination rather than reinsertion, which is in contrast promoted by *rac*-**III**—a quite a surprising result considering their almost identical geometric properties (Table 1).

The high polydispersity observed for entry 1 (Table 2) seems to be related to the low catalyst activity. The corresponding gel-permeation chromatography (GPC) trace (Figure S42) exhibits slight bimodality, which implies the possibility of multiple different catalytically active species being present during the polymerization. Similar trends are indicated by the GPC (Figures S44 and S45) and differential scanning calorimetry (DSC) traces (Figures S49 and S50) of entries 3 and 4. According to the ^{13}C NMR spectra of the polymers, however, none of the catalytically active species produced PE with branches longer than those of methyl groups. The relatively high polydispersities observed, independent of catalyst productivities, indicate that polymer crystallization occurs within the time scale of the polymerization.[33,34]

Curious whether we could vary the branching density or even branching type of PE produced by *rac*-**III** dependent on the activation strategy, we additionally used "Al−H−Al" to activate the precatalyst (entry 5, Table 2). This borate salt containing a homodinuclear Al cation $[i\text{-}Bu_2(DMA)Al]_2(\mu\text{-}H)^+$ (DMA = *N*,*N*-dimethylaniline) was recently established as a well-defined single-component cocatalyst.[25] In fact, PE produced with this species exhibited a lower branch density than PE produced under otherwise equal polymerization conditions (entry 3, Table 2). Apparently, the use of Al−H−Al suppressed β-H elimination reactions, resulting in overall less branched polymers.

This hypothesis is supported by the fact that the productivity of *rac*-**III** was increased by a factor of 2.5 when it was activated with Al−H−Al rather than TIBA/TrBCF—the groups of *Busico* and *Macchioni* recently observed a similar trend for different hafnocene complexes.[35] In addition, the lower average molecular weight of PE produced using Al−H−Al compared to TIBA/TrBCF indicates that the former generally yielded a higher number of catalytically active species. As anticipated, higher degrees of branching caused lower polymer melting transition temperatures for all entries 1−5 (Table 2).

In summary, we established a synthetic route toward two new hafnocene structures, *rac*-**II** and *rac*-**III**, bearing novel structural motives, i.e., dialkoxy bridges of varying lengths. Contrary to our initial expectation that these bridges would prevent the formation of the *meso* isomers of **II** and **III** upon ligand attachment to the central metal atoms, we still detected their presence *via* NMR. Through fractional crystallization, we eventually obtained the desired *rac* hafnocenes, which were characterized using SC-XRD. The bite angles of *rac*-**II** and *rac*-**III** were almost 11° smaller than the bite angle of the "classic" $-SiMe_2-$ bridged *rac*-**I**, leading to more shielded central metal atoms. Consequently, both dialkoxy-bridged complexes resulted in quite low propylene polymerization activities. They were, however, efficient ethylene polymerization catalysts, and both yielded PE with exclusively methyl branches. This is in contrast to long-chain branches that are usually observed in PE produced from metallocene complexes and is—to the best of our knowledge—the first time this phenomenon has been investigated in depth for hafnocene complexes. We assume that the underlying mechanism forming the methyl branches is some kind of restrained chain-walking mechanism relying on β-H elimination, rotation, and subsequent 2,1-reinsertion of the vinyl-terminated alkyl. Variations in polymerization temperature, length of the dialkoxy bridge, and precatalyst activation strategy allowed the control of the branch densities and, thus, the melting transition temperatures of the final polymers. We are currently investigating the influence of the central metal atom and the monomer pressure on the branching structure and are attempting to reduce the length of the dialkoxy bridge to a single methylene unit. Moreover, density functional theory calculations to gain deeper insight into the proposed mechanism are being prepared.

EXPERIMENTAL SECTION

Experimental details are summarized in the Supporting Information.

ASSOCIATED CONTENT

Supporting Information

The Supporting Information is available free of charge at https://pubs.acs.org/doi/10.1021/acs.organomet.4c00459.

General Materials and Methods, NMR-scale polymerizations, synthetic procedures, NMR spectra of all compounds and polymers, GPC and DSC data of all polymers, and SC-XRD data (PDF)

https://doi.org/10.1021/acs.organomet.4c00459
Organometallics 2025, 44, 8−13

Accession Codes

Deposition Numbers 2394313−2394314 contain the supplementary crystallographic data for this paper. These data can be obtained free of charge via the joint Cambridge Crystallographic Data Centre (CCDC) and Fachinformationszentrum Karlsruhe Access Structures service.

AUTHOR INFORMATION

Corresponding Author

Bernhard Rieger − *Wacker-Lehrstuhl für Makromolekulare Chemie, Catalysis Research Center, Technische Universität München, TUM School of Natural Sciences, 85748 Garching, Germany*; orcid.org/0000-0002-0023-884X; Phone: +49 (0)89 289-13571; Email: rieger@tum.de

Authors

Tim M. Lenz − *Wacker-Lehrstuhl für Makromolekulare Chemie, Catalysis Research Center, Technische Universität München, TUM School of Natural Sciences, 85748 Garching, Germany*

Juliana Steck − *Wacker-Lehrstuhl für Makromolekulare Chemie, Catalysis Research Center, Technische Universität München, TUM School of Natural Sciences, 85748 Garching, Germany*

Jin Y. Liu − *Wacker-Lehrstuhl für Makromolekulare Chemie, Catalysis Research Center, Technische Universität München, TUM School of Natural Sciences, 85748 Garching, Germany*

Complete contact information is available at: https://pubs.acs.org/10.1021/acs.organomet.4c00459

Author Contributions

†(T.M.L. and J.S.) These authors contributed equally.

Notes

The authors declare no competing financial interest.

ACKNOWLEDGMENTS

The authors would like to thank Fisnik Avdiu, Nico Chrisam, and Karla Robert for their help with the metallocene syntheses, as well as Fabrizio Napoli and Dr. Raphael Bühler for conducting the LIFDI-MS measurements and Dr. Niklas Rauscher for valuable discussions.

REFERENCES

(1) Sinn, H.; Kaminsky, W.; Vollmer, H. J.; Woldt, R. Living polymers" on polymerization with extremely productive Ziegler catalysts. *Angew. Chem., Int. Ed.* **1980**, *19*, 390−392.

(2) Wild, F. R.; Zsolnai, L.; Huttner, G.; Brintzinger, H. H. ansa-Metallocene derivatives IV. Synthesis and molecular structures of chiral ansa-titanocene derivatives with bridged tetrahydroindenyl ligands. *J. Organomet. Chem.* **1982**, *232*, 233−247.

(3) Kaminsky, W.; Külper, K.; Brintzinger, H. H.; Wild, F. R. Polymerization of propene and butene with a chiral zirconocene and methylalumoxane as cocatalyst. *Angew. Chem., Int. Ed.* **1985**, *24*, 507−508.

(4) Resconi, L.; Cavallo, L.; Fait, A.; Piemontesi, F. Selectivity in Propene Polymerization with Metallocene Catalysts. *Chem. Rev.* **2000**, *100*, 1253−1346.

(5) Kulyabin, P. S.; Izmer, V. V.; Goryunov, G. P.; Sharikov, M. I.; Kononovich, D. S.; Uborsky, D. V.; Canich, J. A. M.; Voskoboynikov, A. Z. Multisubstituted C 2-symmetric ansa-metallocenes bearing nitrogen heterocycles: influence of substituents on catalytic properties in propylene polymerization at higher temperatures. *Dalton Trans.* **2021**, *50*, 6170−6180.

(6) Kulyabin, P. S.; Goryunov, G. P.; Sharikov, M. I.; Izmer, V. V.; Vittoria, A.; Budzelaar, P. H. M.; Busico, V.; Voskoboynikov, A. Z.; Ehm, C.; Cipullo, R.; Uborsky, D. V. ansa-Zirconocene Catalysts for Isotactic-Selective Propene Polymerization at High Temperature: A Long Story Finds a Happy Ending. *J. Am. Chem. Soc.* **2021**, *143*, 7641−7647.

(7) Machat, M. R.; Lanzinger, D.; Pöthig, A.; Rieger, B. Ultrarigid Indenyl-based Hafnocene Complexes for the Highly Isoselective Polymerization of Propene: Tunable Polymerization Performance Adopting Various Sterically Demanding 4-Aryl Substituents. *Organometallics* **2017**, *36*, 399−408.

(8) Schöbel, A.; Herdtweck, E.; Parkinson, M.; Rieger, B. Ultra-Rigid Metallocenes for Highly Iso- and Regiospecific Polymerization of Propene: The Search for the Perfect Polypropylene Helix. *Chem.-Eur. J.* **2012**, *18*, 4174−4178.

(9) Nikulin, M.; Tsarev, A.; Lygin, A.; Ryabov, A.; Beletskaya, I.; Voskoboinikov, A. Palladium-catalyzed arylation of bis (4-bromo-2-methylinden-1-yl) dimethylsilane and related compounds. *Russ. Chem. Bull.* **2008**, *57*, 2298−2306.

(10) Izmer, V. V.; Sorokin, D. A.; Kuz'mina, L. G.; Churakov, A. V.; Howard, J. A. K.; Voskoboynikov, A. Z. Synthesis and molecular structures of zirconium and hafnium complexes bearing dimethylsilandiyl-bis-2,4,6-trimethylindenyl and dimethylsilandiyl-bis-2-methyl-4,6-diisopropylindenyl ligands. *J. Organomet. Chem.* **2005**, *690*, 1067−1079.

(11) Herrmann, W. A.; Rohrmann, J.; Herdtweck, E.; Spaleck, W.; Winter, A. The First Example of an Ethylene-Selective Soluble Ziegler Catalyst of the Zirconocene Class. *Angew. Chem., Int. Ed.* **1989**, *28*, 1511−1512.

(12) Lenz, T. M.; Chiorescu, I.; Napoli, F. E.; Liu, J. Y.; Rieger, B. Aluminum Alkyl Induced Isomerization of Group IV meso Metallocene Complexes. *Angew. Chem., Int. Ed.* **2024**, *63*, No. e202406848.

(13) Stieglitz, L.; Lenz, T. M.; Saurwein, A.; Rieger, B. Perfectly Isotactic Polypropylene upon In Situ Activation of Ultrarigid meso Hafnocenes. *Angew. Chem., Int. Ed.* **2022**, *61*, No. e202210797.

(14) Möhring, P. C.; Coville, N. J. Group 4 metallocene polymerisation catalysts: quantification of ring substituent steric effects. *Coord. Chem. Rev.* **2006**, *250*, 18−35.

(15) Shaltout, R. M.; Corey, J. Y.; Rath, N. P. The X-ray crystal structures of the ansa-metallocenes, Me2C (C5H4) 2MCl2 (M= Ti, Zr and Hf). *J. Organomet. Chem.* **1995**, *503*, 205−212.

(16) Shapiro, P. J. The evolution of the ansa-bridge and its effect on the scope of metallocene chemistry. *Coord. Chem. Rev.* **2002**, *231*, 67−81.

(17) Lenz, T. M.; Rieger, B. Isotactic polypropylene produced by rac/meso mixtures of hafnocene complexes through selective rac activation. *J. Polym. Sci.* **2024**, *62*, 5257−5264.

(18) Bryliakov, K. P.; Talsi, E. P.; Voskoboynikov, A. Z.; Lancaster, S. J.; Bochmann, M. Formation and Structures of Hafnocene Complexes in MAO- and AlBui3/CPh3[B(C6F5)4]-Activated Systems. *Organometallics* **2008**, *27* (23), 6333−6342.

(19) Meinhard, D.; Wegner, M.; Kipiani, G.; Hearley, A.; Reuter, P.; Fischer, S.; Marti, O.; Rieger, B. New nickel (II) diimine complexes and the control of polyethylene microstructure by catalyst design. *J. Am. Chem. Soc.* **2007**, *129*, 9182−9191.

(20) Gabriel, C.; Kokko, E.; Löfgren, B.; Seppälä, J.; Münstedt, H. Analytical and rheological characterization of long-chain branched metallocene-catalyzed ethylene homopolymers. *Polymer* **2002**, *43*, 6383−6390.

(21) Wang, W.-J.; Yan, D.; Zhu, S.; Hamielec, A. E. Kinetics of long chain branching in continuous solution polymerization of ethylene using constrained geometry metallocene. *Macromolecules* **1998**, *31*, 8677−8683.

(22) Rappé, A.; Skiff, W.; Casewit, C. Modeling metal-catalyzed olefin polymerization. *Chem. Rev.* **2000**, *100*, 1435−1456.

(23) Kokko, E.; Malmberg, A.; Lehmus, P.; Löfgren, B.; Seppälä, J. V. Influence of the catalyst and polymerization conditions on the long-chain branching of metallocene-catalyzed polyethenes. *J. Polym. Sci. Part A. Polym. Chem.* **2000**, *38*, 376−388.

(24) Hamielec, A. E.; Soares, J. B. Polymerization reaction engineering—metallocene catalysts. *Prog. Polym. Sci.* **1996**, *21*, 651−706.
(25) Zaccaria, F.; Zuccaccia, C.; Cipullo, R.; Budzelaar, P. H.; Vittoria, A.; Macchioni, A.; Busico, V.; Ehm, C. Methylaluminoxane's molecular cousin: A well-defined and "complete" al-activator for molecular olefin polymerization catalysts. *ACS Catal.* **2021**, *11*, 4464−4475.
(26) Guan, Z.; Cotts, P.; McCord, E.; McLain, S. Chain walking: a new strategy to control polymer topology. *Science* **1999**, *283* (5410), 2059−2062.
(27) Johnson, L. K.; Killian, C. M.; Brookhart, M. New Pd (II)-and Ni (II)-based catalysts for polymerization of ethylene and. alpha.-olefins. *J. Am. Chem. Soc.* **1995**, *117*, 6414−6415.
(28) Killian, C. M.; Tempel, D. J.; Johnson, L. K.; Brookhart, M. Living polymerization of α-olefins using NiII−α-diimine catalysts. Synthesis of new block polymers based on α-olefins. *J. Am. Chem. Soc.* **1996**, *118*, 11664−11665.
(29) Guan, Z. Control of Polymer Topology by Chain-Walking Catalysts. *Chem.-Eur. J.* **2002**, *8*, 3086−3092.
(30) Zhang, Y.; Zhang, Y.; Jian, Z. A comprehensive picture on chain walking olefin polymerization. *Polymer* **2023**, *265*, 125578.
(31) Gates, D. P.; Svejda, S. A.; Oñate, E.; Killian, C. M.; Johnson, L. K.; White, P. S.; Brookhart, M. Synthesis of branched polyethylene using (α-diimine) nickel (II) catalysts: influence of temperature, ethylene pressure, and ligand structure on polymer properties. *Macromolecules* **2000**, *33*, 2320−2334.
(32) Wu, R.; Lenz, T. M.; Stieglitz, L.; Galois, R.; Zhao, R.; Rupper, P.; Lehner, S.; Jovic, M.; Neels, A.; Gaan, S.; et al. Controlling polyethylene branching via surface confinement of Ni complexes. *J. Catal.* **2023**, *426*, 270−282.
(33) Guo, Q. *Polymer morphology: principles, characterization, and processing*; John Wiley & Sons, 2016.
(34) Flory, P. J. *Principles of polymer chemistry*; Cornell University Press, 1953.
(35) Urciuoli, G.; Zaccaria, F.; Zuccaccia, C.; Cipullo, R.; Budzelaar, P. H.; Vittoria, A.; Ehm, C.; Macchioni, A.; Busico, V. Cocatalyst effects in Hf-catalysed olefin polymerization: taking well-defined Al−alkyl borate salts into account. *Dalton Trans.* **2024**, *53*, 2286−2293.

https://doi.org/10.1021/acs.organomet.4c00459
Organometallics 2025, 44, 8−13